

Supplemental Figures and Table

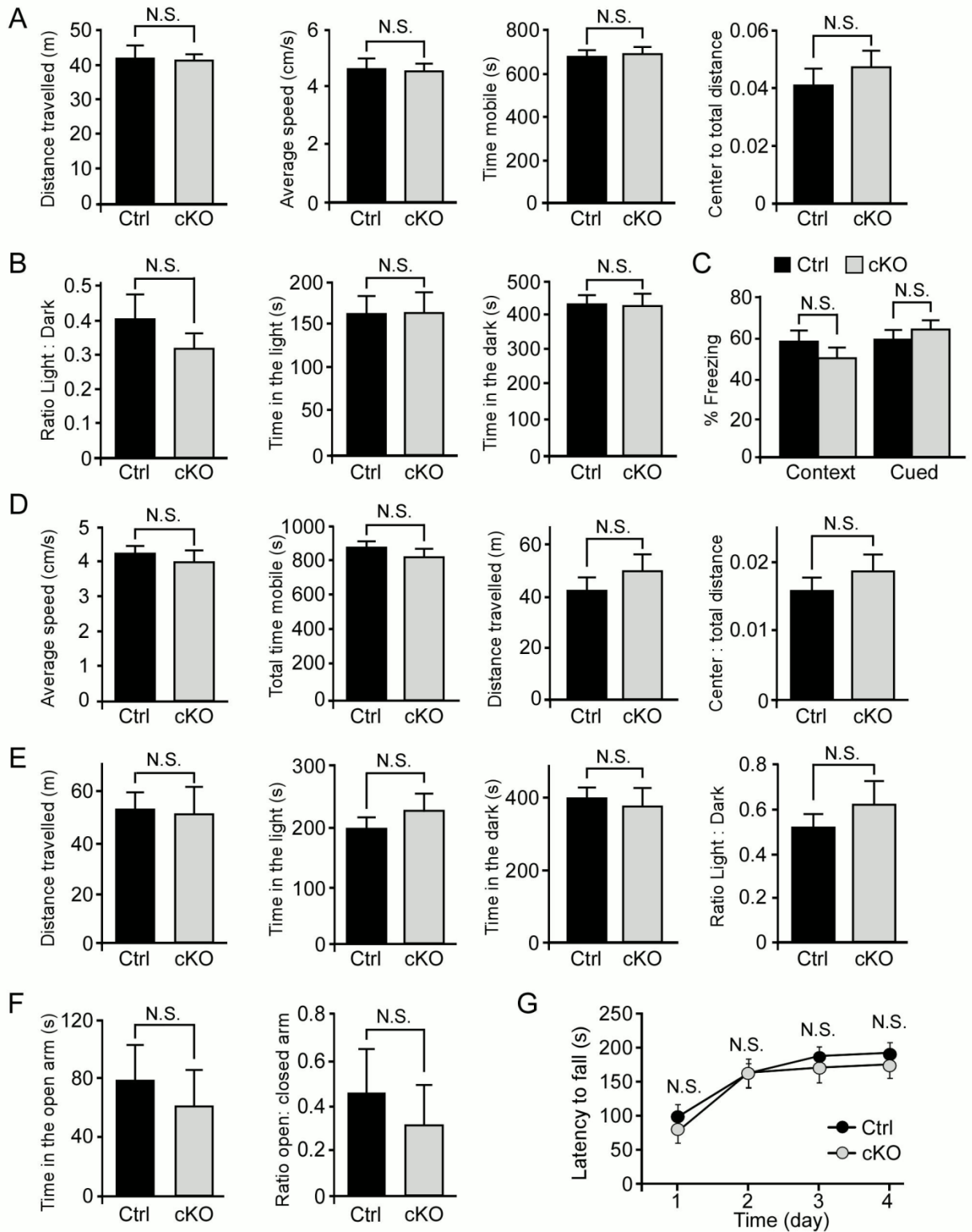


Figure S1. Analyses of Neurobehavior in Control and LRP6 Neuronal Knockout Mice at 6 and 22 Months of Age, Related to Figure 1

(A) Analyses of anxiety-related behaviors in control (Ctrl) and Lrp6 cKO (cKO) mice at 6 months of age (n=13-15 mice per genotype) assessed by open field tests. The total distance traveled, average speed, time spent mobile, and ratio of time spent in the center quadrants to total distance traveled in the open field apparatus are shown. In this figure, data are presented as mean \pm SEM. N.S., not significant.

(B) Analyses of anxiety-related behaviors in Ctrl and Lrp6 cKO mice at 6 months of age (n=13-15 mice per genotype) assessed by light/dark exploration tests. The time spent in the light chamber, time spent in the dark chamber, and ratio of time spent in light to dark chambers are shown. N.S., not significant.

(C) The cognitive function of Ctrl and Lrp6 cKO mice (n=13-15 mice per genotype) at 6 months of age examined by fear conditioning tests. The percentage of the time with freezing behavior in response to stimulus during contextual or cued memory tests is shown. N.S., not significant.

(D) Analyses of anxiety-related behaviors in Ctrl and Lrp6 cKO mice at 22 months of age (n=10-11 mice per group) assessed by open field tests. The average speed, time spent mobile, total distance traveled, and ratio of time spent in the center quadrants to total distance traveled in the open field apparatus are shown.. N.S., not significant.

(E) Analyses of anxiety-related behaviors in Ctrl and Lrp6 cKO mice at 22 months of age (n=10-11 mice per group) assessed by light/dark exploration tests. The total distance traveled, time spent in the light chamber, time spent in the dark chamber, and ratios of time spent in light to dark chambers are shown. N.S., not significant.

(F) Analyses of anxiety-related behaviors in Ctrl and Lrp6 cKO mice at 22 months of age (n=10-11 mice per group) assessed by elevated plus maze test. Total time in the open arms and ratio of time spent in open to closed arms are shown. N.S., not significant.

(G) The locomotor activity and motor learning in Ctrl and Lrp6 cKO mice at 22 months of age (n=10-11 mice per group) examined by rotarod test. N.S., not significant.

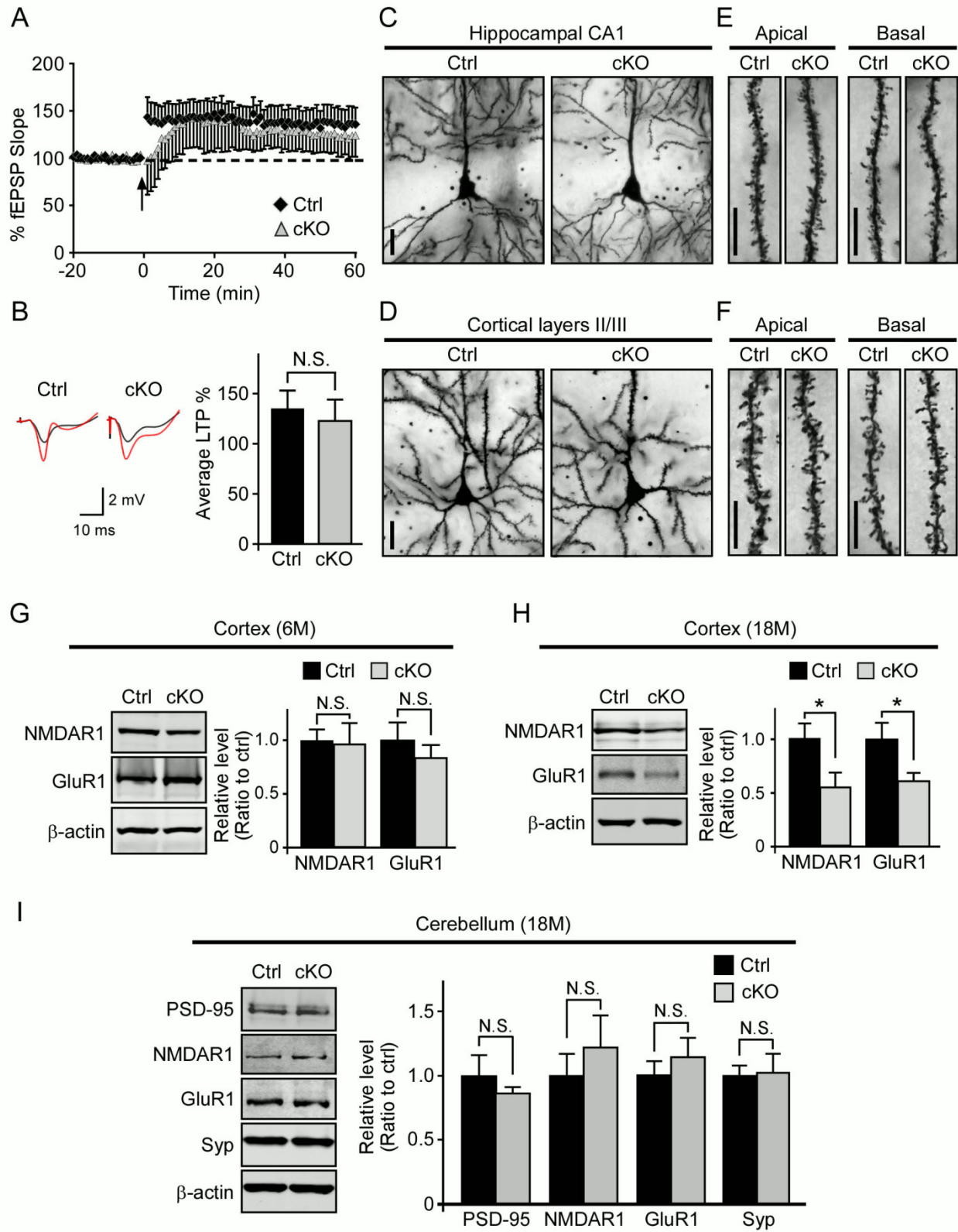


Figure S2. Analyses of Long-term Plasticity, Dendritic Spine Density, and Synaptic Integrity in Control and LRP6 Neuronal Knockout Mice, Related to Figures 1 and 2

(A) Normal hippocampal LTP in the CA1 region of Lrp6 cKO (cKO) (n=12) mice at 6 months of age compared to control (Ctrl) (n=16) mice. Changes in fEPSP slope were expressed as a percentage of baseline. Data represent mean \pm SEM.

(B) Representative traces before (black) and after (red) high frequency stimulation from the recordings of Ctrl and Lrp6 cKO mice. Averages of the last 5 min of recording.

(C and D) Representative Golgi-impregnated neurons in hippocampal CA1 region (C) and cortical layer II/III (D) from Ctrl and Lrp6 cKO mice at 6 months of age. Scale bars, 10 μ m.

(E and F) Representative apical oblique and basal shaft dendrites from hippocampal CA1 region (E) and cortical layers II/III (F) of Ctrl and Lrp6 cKO mice at 6 months of age. Scale bars, 10 μ m.

(G) NMDAR1 and GluR1 levels in the cortex of Ctrl and Lrp6 cKO mice at 6 months of age (n=4-5 per genotype) examined by Western blot analysis. The densitometric quantification of Western blot is shown as mean \pm SEM.

(H) NMDAR1 and GluR1 levels in the cortex of Ctrl and Lrp6 cKO mice at 18 months of age (n=5-7 per genotype) examined by Western blot analysis. The densitometric quantification of Western blot is shown as mean \pm SEM. *p < 0.05.

(I) The levels of synaptic markers in the cerebellum of Ctrl and Lrp6 cKO mice at 18 months of age (n=6 per genotype) examined by Western blot analysis. Syp, Synaptophysin. The densitometric quantification of Western blot is shown as mean \pm SEM. N.S., not significant.

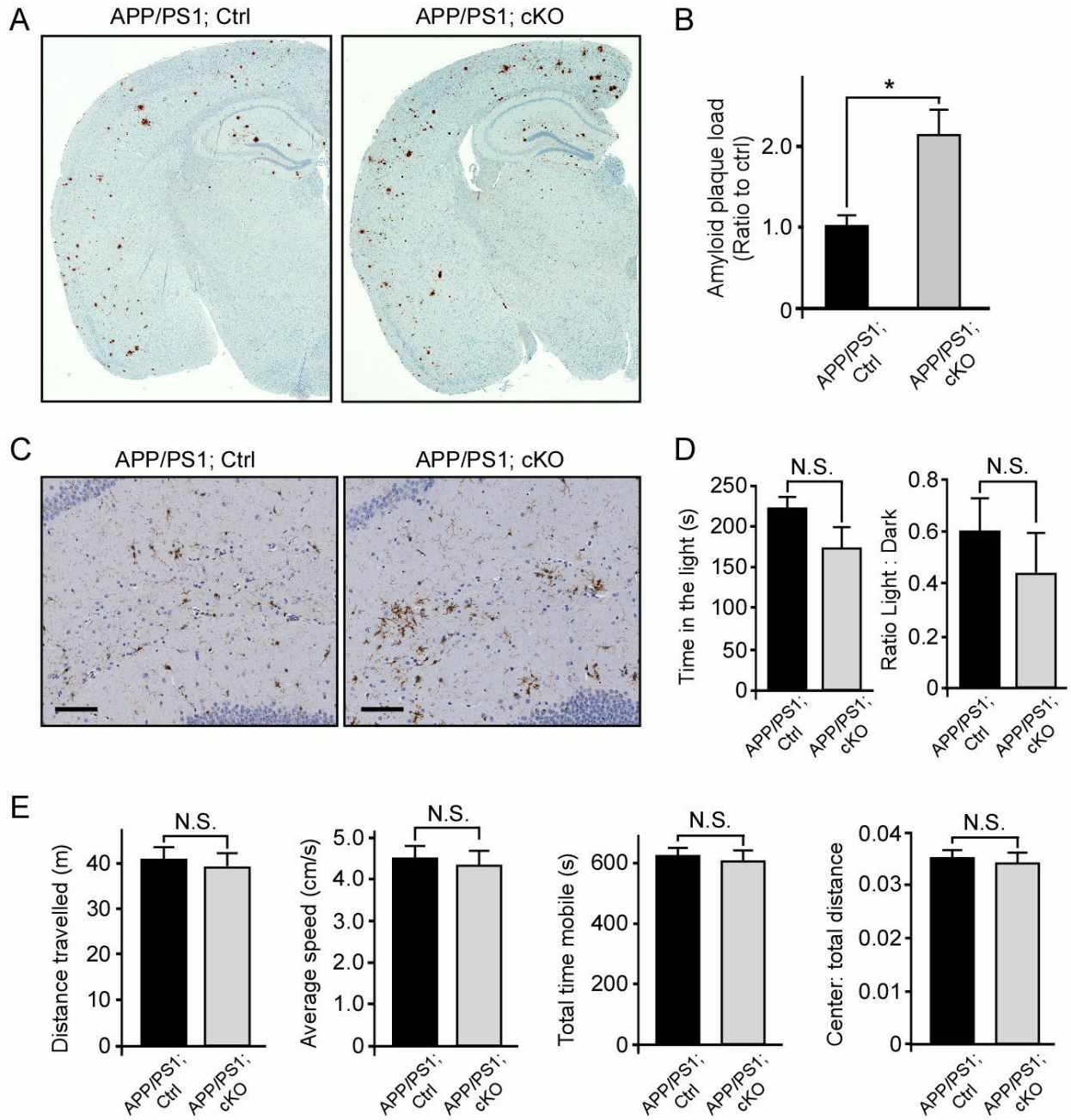


Figure S3. Amyloid Deposition, Neuroinflammatory Response and Anxiety Behaviors in APP/PS1 Mice with or without Neuronal LRP6 Deletion, Related to Figure 4

(A and B) Brain sections from APP/PS1; Ctrl and APP/PS1; cKO mice (n=5 per group) at 6 months of age immunostained for A β . Scale bar, 100 μ m. (B) The percentage of area covered by plaques in cortex was quantified, and the plaque load was normalized to that of APP/PS1; Ctrl mice. Values are mean \pm SEM. *p < 0.05.

(C) Hemi-brain sections from APP/PS1; Ctrl and APP/PS1; cKO mice at 9 months of age immunostained with Iba1 antibody, a marker of microgliosis. Representative pictures of hippocampus are shown. Scale bar, 100 μ m.

(D) The analyses of anxiety-related behaviors in APP/PS1; Ctrl and APP/PS1; cKO mice (n=14 mice per group) at 12 months of age assessed by open field tests. Total distance traveled, average speed, time spent mobile, and ratio of time spent in the center quadrants to total distance traveled in the open field are shown. N.S., not significant.

(E) Anxiety-related behaviors in APP/PS1; Ctrl and APP/PS1; cKO mice at 12 months of age assessed by light/dark exploration tests. The time spent in the light chamber and ratio of time spent in light to dark chambers (n=14 mice per group) are shown. N.S., not significant.

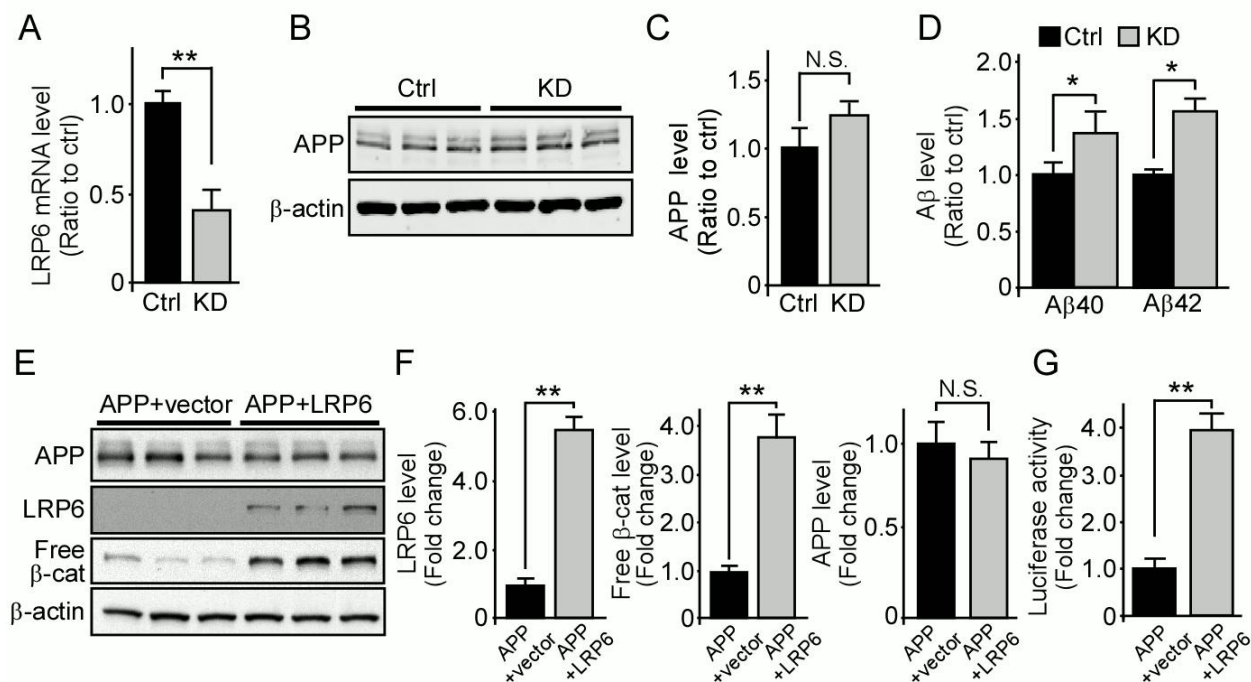


Figure S4. Modulation of LRP6 Affects Wnt Signaling, Related to Figure 5

(A) The mRNA levels of LRP6 in N2a-APP cells expressing control shRNA (Ctrl) or LRP6 shRNA (KD) examined by real-time PCR analysis. Results were normalized to β-actin levels. Values are mean ± SD. *p < 0.05.

(B and C) The APP levels in N2a-APP cells expressing control shRNA (Ctrl) or LRP6 shRNA (KD) examined by Western blot analysis. Densitometric analyses of Western blots are shown in (C). N.S., not significant.

(D) The Aβ40 or Aβ42 levels in the medium of N2a-APP cells expressing control shRNA (Ctrl) or LRP6 shRNA (KD) examined by ELISA. All measurements were normalized to protein concentrations in the cell lysates. Values are mean ± SD. *p < 0.05.

(E and F) The levels of APP, LRP6 and free β-catenin in HEK293 cells co-transfected with APP together with pcDNA or LRP6/Mesd examined by Western blot analysis. Free β-catenin levels were evaluated by GST-E-Cadherin pull-down, followed by Western blot analysis.

Densitometric analyses of Western blots are shown in (F). Values are mean \pm SD. **p < 0.01; N.S., not significant.

(G) The levels of Wnt signaling in HEK293 cells co-expressing TOPFlash reporter and APP together with pcDNA or LRP6/Mesd examined by TOPFlash luciferase assay. Values are mean \pm SD. **p < 0.01.

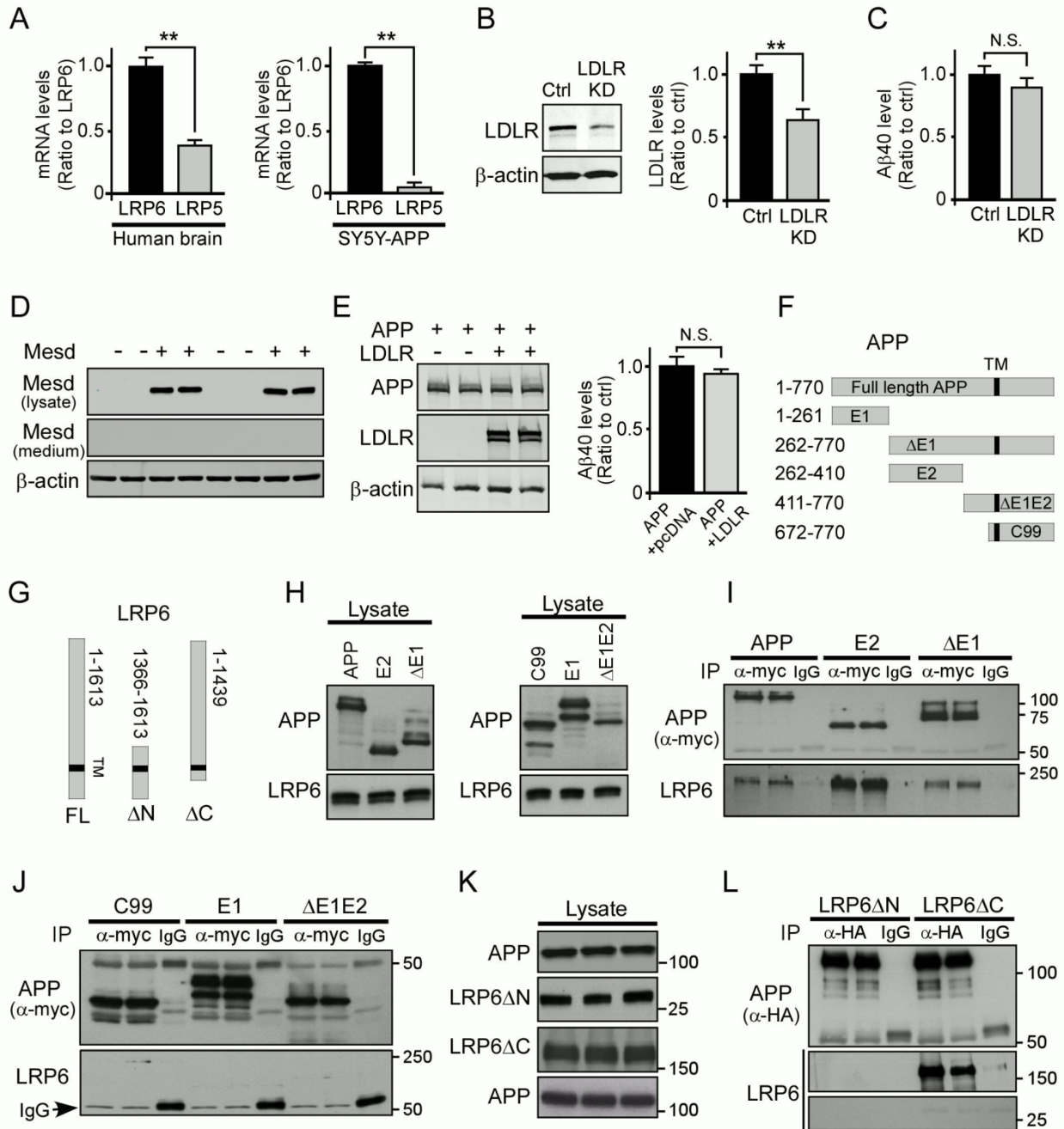


Figure S5. The APP E2 Domain Interacts with LRP6 Extracellular Domain, Related to Figure 5

(A) LRP5 and LRP6 mRNA levels in human brain tissue and SH-SY5Y-APP cells quantified by real-time PCR. The standard curves for human LRP5 and LRP6 was derived from the serial dilutions of plasmids with known concentration. The logarithms (base 10) of concentrations were plotted against threshold cycle (Ct), and the levels of LRP5 and LRP6 were calculated using its corresponding standard curves. Values are mean \pm SD. ** $p < 0.01$.

(B and C) The levels of LDLR and β -actin in N2a-APP cells expressing control and LDLR siRNA examined by Western blot analysis. (C) The level of A β 40 in the medium was evaluated by ELISA. N2a-APP cells were transfected with control or LDLR siRNA. 48 h post co-transfection, cell medium were replaced with Opti-MEN medium and incubated for 12 h. The A β 40 level in the medium was normalized to total protein levels in cell lysates. N.S., not significant.

(D) The levels of Mesd in HEK293 cells with or without overexpressing flag-tagged Mesd and in the concentrated medium analyzed by Western blot.

(E) The level of A β 40 in the medium of HEK293 cells overexpressing APP with either vector or HA-tagged LDLR was evaluated by ELISA. The levels of LDLR, APP and β -actin in the cell lysates were analyzed by Western blot. HEK293 cells were co-transfected with APP together with pcDNA or LDLR. 24 h post co-transfection, cell medium were replaced with DMEM medium containing 1% FBS and incubated for 12 h. The A β 40 level in the concentrated medium was quantified after normalization with total protein levels in the cell lysates. Values are mean \pm SD. * $p < 0.05$.

(F and G) Schematic diagrams of APP and LRP6 constructs used in this study.

(H) Western blot of LRP6 and different APP fragments used as inputs of immunoprecipitation.

(I and J) LRP6 co-immunoprecipitated with full-length APP, APP-E2 and APP- Δ E1, but not C99, APP-E1 and APP- Δ E1E2. HEK293 cells were co-transfected with plasmids expressing various myc-APP and HA-LRP6 together with Mesd. Cell lysates were immunoprecipitated with an anti-myc antibody for APP, and probed with an anti-HA antibody for LRP6.

(K and L) LRP6 extracellular domain is required for the APP-LRP6 interaction. HEK293 cells were co-transfected with plasmids expressing HA-APP, LRP6 Δ C-VSVG or myc-LRP6 Δ N together with Mesd. Cell lysates were subjected to immunoprecipitation with anti-HA antibody against APP, and probed with anti-LRP6 or anti-myc antibodies.

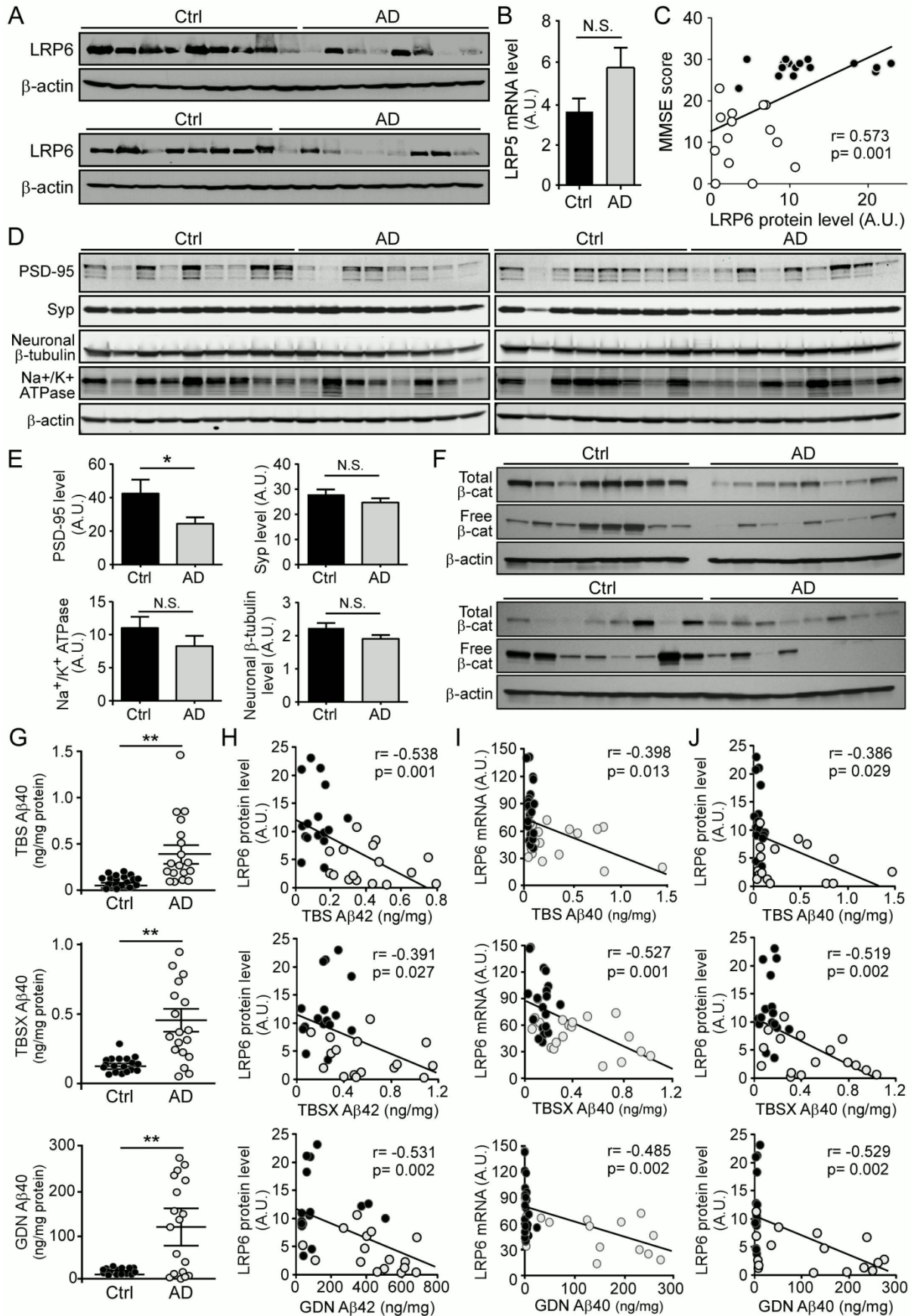


Figure S6. The Levels of LRP6-mediated Wnt Signaling and its Correlation with A β Levels in Human Control and AD Brain Tissues, Related to Figure 6

(A) LRP6 protein levels in human control (n=17) and AD (n=17) brain tissues examined by Western blot analysis.

(B) LRP5 mRNA levels in human control (n=20) and AD (n=18) brain tissues quantified by real-time PCR. Results were normalized to β -actin levels and presented in relative units. In the following figures, data are shown as scatterplots in which each symbol represents an individual case. A.U., arbitrary unit. Data represent mean \pm SEM. **p < 0.01.

(C) Correlation between LRP6 protein levels (Figures 6B and S6A) and mini-mental state examination (MMSE) score of human control (dark circles) and AD (light circles) brain tissues (r represents the correlation coefficient; p is significance).

(D and E) Synaptic markers (PSD-95 and Synaptophysin), sodium/potassium ATPase, a critical membrane marker and neuron-specific β -tubulin in control (n=17) and AD (n=17) brain tissues examined by Western blot analysis and quantified.

(F) The levels of total and free β -catenin in human control (n=16) and AD (n=16) brain tissues examined by Western blot analysis. Free β -catenin levels were evaluated by GST-E-Cadherin pull-down, followed by Western blot analysis.

(G) A β 40 levels in TBS, TBSX, and GDN fractions of human control (n=20) and AD (n=18) brain tissues. Data are shown as scatterplots in which each symbol represents an individual case. Data represent mean \pm SEM. **p < 0.01.

(H) Correlation between LRP6 protein levels (Figures 6B and S6A) and A β 42 levels (Figure 6G) in various extraction fractions (TBS, TBSX or GDN) in human control (dark circles) and AD (light circles) brain tissues (r represents the correlation coefficient; p is significance). In this and following figure, LRP6 protein levels are presented in relative units. A.U., arbitrary unit.

(I) Correlation between LRP6 mRNA levels (Figure 6A) and A β 40 levels (Figure S6G) in various extraction fractions (TBS, TBSX or GDN) in human control (dark circles) and AD (light circles) brain tissues (r represents the correlation coefficient; p is significance).

(J) Correlation between LRP6 protein levels (Figures 6B and S6A) and A β 40 levels (Figure S6G) in various extraction fractions (TBS, TBSX or GDN) in human control (dark circles) and AD (light circles) brain tissues (r represents the correlation coefficient; p is significance).

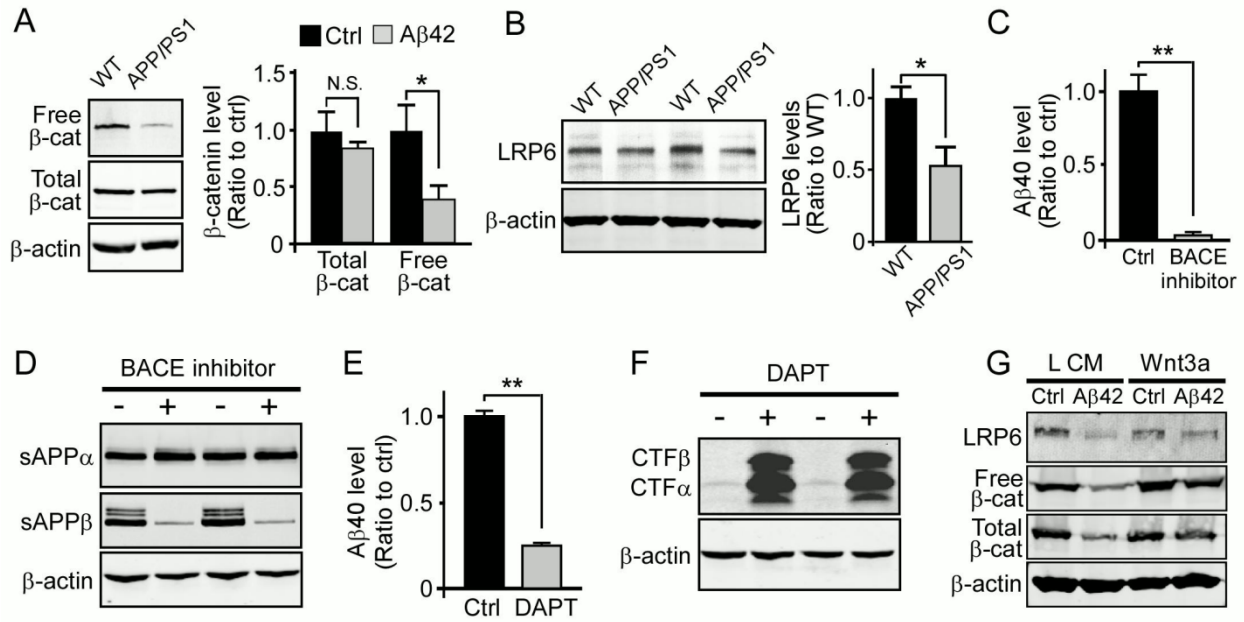


Figure S7. The Levels of LRP6-mediated Wnt Signaling is Down-regulated in APP/PS1 Mouse Brains and in Neuronal Cells upon Aβ Treatment, Related to Figure 7

(A and B) The levels of total and free β-catenin (β-cat) and LRP6 in the hippocampus of wild-type (WT) mice and APP/PS1 mice at 12 months of age (n=4-5/per genotype) examined by Western blot analysis. Free β-catenin levels were analyzed by GST-E-Cadherin pull-down assay. Data represent mean ± SEM. N.S., not significant; *p < 0.05.

(C-F) The levels of soluble APP fragments (sAPPα and sAPPβ) or APP-CTFs (CTFα and CTFβ) in N2a-APP cells treated with or without BACE inhibitor (β-secretase inhibitor IV, 2 μM) or γ-secretase inhibitor (DAPT, 10 μM) examined by Western blot analysis. The levels of Aβ40 in the media were evaluated by ELISA (C and E). Data represent mean ± SD. **p < 0.01.

(G) The levels of LRP6, total and free β-catenin in SH-SY5Y cells treated with 5 μM Aβ42 oligomers in the presence or absence of Wnt3a ligands examined by Western blot analysis. L CM, L cell conditioned medium; Wnt3a, Wnt3a conditioned medium.

Table S1: Characteristics of Examined Individuals, Related to Figure 6

Characteristics	Ctrl (n=20)	AD (n=18)
Age (yrs)	85.1 ± 5.7	84.2 ± 4.1
Sex (M/F)	9/11	7/11
Postmortem interval (h)	3.0 ± 0.9	3.3 ± 0.8
Braak NFT stage	0-2	5-6
<i>APOE</i> ε4 carriers (%)	25	56 ^a
MMSE total score	28.2 ± 1.8	11.5 ^b ± 6.6

Data is expressed as mean ± s.d.

MMSE, mini-mental state examination; NFT, neurofibrillary tangle

^a*APOE* genotype examined in n=16 individuals.

^bMMSE scores obtained from n=17 individuals.

Supplemental Experimental Procedures

Animals and Tissue Preparation

LRP6 forebrain neuronal knockout mice were generated by breeding the *Lrp6*^{lox/lox} mice with CaMKII-Cre mice (Jackson Labs) in which the Cre recombinase is expressed broadly in most excitatory neurons of the forebrain, including the hippocampus and the cortex. *Lrp6*^{lox/lox} mice were backcrossed with C57BL/6 mice for 10 generations before breeding to CaMKII-Cre mice. LRP6 conditional knockout (*Lrp6* cKO) mice (*Lrp6*^{lox/lox}, CaMKII-Cre) and littermate control (Ctrl) mice (*Lrp6*^{lox/lox}) were used for analysis. To generate APP/PS1; *Lrp6* cKO mice, we bred APP/PS1; *Lrp6*^{lox/lox} mice with *Lrp6*^{lox/lox}, CaMKII-Cre mice. APP/PS1; *Lrp6*^{lox/lox}, CaMKII-Cre (APP/PS1; cKO) and littermate control APP/PS1; *Lrp6*^{lox/lox} (APP/PS1; Ctrl) mice were used for analysis. For tissue preparation, mice were transcardially perfused with saline. Different regions of brain tissues (cortex, hippocampus and cerebellum) were snap-frozen in liquid nitrogen and stored at -80°C. For biochemical analysis, the brain tissues were homogenized on ice and the resulting supernatants were used for Western blot analysis. In some experiments, the membrane fraction was prepared as described (Shinohara et al., 2010). In brief, brain samples were homogenized in tissue homogenization buffer (THB; 0.25 M sucrose, 20 mM Tris-HCl, pH 7.4, 1 mM EDTA, 1 mM EGTA) containing protease inhibitor mixture. After centrifugation at 1600g for 5 min at 4°C, the postnuclear supernatant was further centrifuged at 100,000g for 60 min at 4°C; the resulting supernatants were used as soluble fractions. After washing, the remaining pellets were re-suspended, solubilized and used as the membrane fraction.

Cell Culture

Human neuroblastoma SH-SY5Y cells (ATCC), SH-SY5Y-APP (a kind gift from Dr. Steven Wagner (University of California, San Diego, CA)), and HEK293 cells were cultured in Dulbecco's modified essential medium (DMEM) supplemented with 10% fetal bovine serum (FBS) and maintained at 37°C in humidified air containing 5% CO₂. Mouse neuroblastoma N2a cells stably expressing APP were maintained in DMEM/Opti-MEM (1:1) containing 5% FBS and 2 mM L-glutamine. Primary mouse cortical neurons were obtained from 16-18 d embryos of wild-type mice as previous described (Liu et al., 2010). Cultures were grown in neurobasal medium supplemented with B27, 0.5 mM glutamine, penicillin and streptomycin.

Golgi Staining and Dendritic Spine Analysis

Golgi staining was performed using the FD Rapid Golgi Stain kit (FD Neuro Technologies) as described (Liu et al., 2010). Freshly dissected brains were immersed in solution A and B in FD Rapid Golgi Stain kit for 2 weeks at room temperature and then transferred to solution C for 3-5 d at 4°C. Brains were sliced with a cryostat (LEICA CM3050 S, Leica) at a thickness of 80 µm. The Golgi-stained neurons and dendritic segments in hippocampal CA1 and layer II/III of the cortex were imaged with the Axio Imager Z1 microscope (Carl Zeiss). The Extended Focus module was used to compress Z-stack images into one single image. The pyramidal neurons in cortical layers II/III and in the CA1 region of the hippocampus were analyzed. Ten neurons were randomly selected per region in each mouse (n=5 per genotype). Two segments (average 70 µm) were randomly chosen per neuron from both the apical oblique and basal shaft (BS) dendrites, and the numbers of spines were counted in a blinded fashion using Metamorph software (Molecular Devices).

Constructs, Lentivirus-delivered RNA Interference and A β Preparation

To generate HA-LRP6, human pCS-Myc-hLRP6 cDNA (kindly provided by Dr. Christof Niehrs, Heidelberg, Germany) was used as a template for PCR and the PCR products were then subcloned into the BamH1/XbaI sites of mLRP4T100 backbone as previously described (Liu et al., 2009). We generated N-terminal signal peptide and C-terminal myc-tagged deletion constructs of APP as follows: APP-E1 (residues 1-261aa), APP-E2 (residues 262-410aa), APP- Δ E1 (residues 262-770aa), APP- Δ E1E2 (residues 411-770aa). Myc-LRP6 Δ N (hLRP6 mutant lacking extracellular domain) was described previously (Li et al., 2006). VSVG-LRP6 Δ C (hLRP6 mutant lacking cytoplasmic tail) was kindly provided by Dr. X. He (Tamai et al., 2000). Constitutively active β -catenin (β -catenin deltaN90) plasmid (Guo et al., 2012) was obtained from Addgene (plasmid 36985). LRP6 specific shRNAs were purchased from Sigma, and lentiviruses were produced in the Viral Vectors Core facility at Washington University School of Medicine. In brief, 293T cells were transfected with pLKO.1-derived constructs together with the pHR8.2 and pCMV-VSV-G packaging systems as previously described (Stewart et al., 2003). pLKO.1 shRNA was used as control. Control siRNA and mouse LDLR siRNA were obtained from Sigma. Cortical neurons were infected with lentivirus at 10-12 d *in vitro*. Western blot analysis or immunofluorescence staining was performed 2-4 d post infection. A β oligomers were prepared with help from Dr. Terrone Rosenberry and Dr. William Tay as previously described (Tay et al., 2012).

Extracellular Field Recording from Acute Hippocampal Slices

Horizontal hippocampal slices of 400 μ m thickness from littermate mice were prepared using a Leica LS1000 vibrating microtome in ice cold cutting solution containing (in mM) sucrose 110, NaCl 60, KCl 3, NaH₂PO₄ 1.25, NaHCO₃ 28, sodium ascorbate acid 0.6, glucose 5, MgCl₂ 7, CaCl₂ 0.5. Slices were then transferred to a holding chamber (Scientific Designs Inc.) which

contained oxygenated artificial cerebrospinal fluid (aCSF) of the following composition (in mM) NaCl 126, KCl 2.5, NaH₂PO₄ 1.25, MgCl₂ 2, CaCl₂ 2, NaHCO₃ 26, glucose 10, pyruvic acid 2, ascorbic acid 0.4. Slices were left to recover for at least 90 min at room temperature prior to recording. Slices from old and young animals were positioned on multi-electrode arrays (MED-64 system) or interface chamber (Brain Slice Chamber-1, Automate Scientific), respectively, and perfused with aCSF at a rate of 1 ml/min, equilibrated with 95% O₂ and 5% CO₂ at 22°C.

Field excitatory post-synaptic potentials (fEPSPs) were invoked through stimulation of the Schaffer collaterals and obtained from area CA1 stratum radiatum. fEPSPs obtained from slices of old animals were recorded with MED-64 system and Mobius software (Alpha MED Scientific Inc). Slices obtained from young animals were recorded with a glass microelectrode filled with aCSF (2-4 mΩ) and pClamp 10.2 software (Axon instruments). fEPSPs were evoked through stimulation of the Schaffer collaterals using a 0.1 msec biphasic pulse. After a consistent response to a stimulus was established, threshold for evoking fEPSPs was determined and the stimulus was increased incrementally until the maximum amplitude of the fEPSP was reached (I/O curve). All other stimulation paradigms were induced at the same half-maximal stimulus strength, defined as 50% of the stimulus used to produce the maximum fEPSP amplitude, as determined by the I/O curve, for each individual slice. After a stable baseline recording of 20 min was established, LTP was induced using high-frequency stimulation (HFS), which consisted of 100 pulses at 100 Hz applied 3 times with one-minute intervals. fEPSPs were monitored every 30 sec for 60 min following HFS. Potentiation was calculated as the percent increase of the mean fEPSP descending slope following HFS and normalized to the mean fEPSP descending slope of baseline recordings.

Preparation of Brain Homogenates

Mouse brain tissues and human postmortem brain tissues were processed through sequential extraction as described (Youmans et al., 2011). Frozen brain tissues were homogenized with TBS, and centrifuged at 100,000g for 60 min at 4°C (TBS-soluble fraction). Pellets were re-suspended in TBS buffer containing 1% Triton X-100 (TBSX) and mixed gently by rotation at 4°C for 30 min, followed by a second centrifugation at 100,000g for 60 min (TBSX-soluble fraction). The TBSX-insoluble pellet was re-suspended with 5M guanidine, mixed by rotation at room temperature overnight, and centrifuged at 16,000g for 30 min (GDN-soluble fraction). For measurement of endogenous A β in the brain, the diethylamine (DEA) extraction method was used as described (Schmidt et al., 2005; Shinohara et al., 2010). Briefly, the brain homogenate in THB (0.25 M sucrose, 20 mM Tris-HCl, pH 7.4, 1 mM EDTA, 1 mM EGTA) containing protease inhibitor cocktail was further homogenized with an equal volume of cold 0.4% DEA and 100 mM NaCl on ice. After centrifugation at 100,000g for 60 min at 4°C, the supernatant was neutralized with a 1/10 volume of 0.5 M Tris-base (pH 6.8) and applied to the A β ELISA.

ELISA Assays

A β levels were determined by ELISA (Das et al., 2012) with end-specific mAbs 2.1.3 (human A β _{x-42} specific) and mAb 13.1.1 (human A β _{x-40} specific) for capture and HRP-conjugated mAb Ab5 (human A β ₁₋₁₆ specific) for detection. Murine IL-1 β , and TNF- α were measured using a DuoSet ELISA kit (R&D Systems) according to manufacturer's instructions.

Immunohistochemical Staining and Analysis

Paraffin embedded sections were immunostained using pan-A β (A β 33.1.1; human A β 1-16 specific), anti-GFAP (BioGenex), and anti-ionized calcium-binding adaptor molecule 1 (Iba-1)

(Wako) antibodies (Chakrabarty et al., 2010). Immunohistochemically stained sections were captured using the ImageScope XT image scanner (Aperio Technologies) and analyzed using the ImageScope software. The intensity of GFAP and Iba-1 staining in the hippocampus were calculated using the Positive Pixel Count program available with the ImageScope software (Aperio Technologies) (Chakrabarty et al., 2010). All of the above analyses were performed in a blinded manner.

Behavioral Studies

The contextual fear conditioning test was conducted in a sound attenuated chamber with a grid floor capable of delivering an electric shock. Freezing was measured with an overhead camera and FreezeFrame software (Actimetrics). Mice were initially placed into the chamber and undisturbed for 2 min, during which time baseline freezing behavior was recorded. An 80-dB white noise served as the conditioned stimulus (CS) and was presented for 30 sec. During the final 2 sec of this noise, mice received a mild foot shock (0.5 mA), which served as the unconditioned stimulus (US). After 1 min, another CS-US pair was presented. The mouse was removed 30 sec after the second CS-US pair. To assess contextual learning, the animals were placed back into the training context 24 h post-training and scored for freezing for 5 min. To assess cued learning, the animals were then placed in a different context (novel odor, cage floor and visual cues) for 3 min and then the auditory CS was presented and freezing was recorded for another 3 min. Baseline freezing behavior obtained during training was subtracted from the context or cued tests to control for animal variability. For the rotarod test, mice were placed on the rotating rod with a linear increase in rotation speed from 4 to 40 RPM and ability to maintain balance on a rotating cylinder was measured. Mice were subjected to 4 trials per day for 4 consecutive days, and the latency to remain on the rotarod was averaged for each trial. For

open-field analysis, the animals were placed in the open field (40 x 40 x 30 cm) chamber for 15 min in standard room-lighting conditions. Activity in the open field was monitored by an overhead camera to track movement with AnyMaze software (Stoelting Co.). Mice were analyzed for multiple measures, including total distance traveled, average speed, and the time spent in the center of the chamber (digitally designated by an 8 × 8 cm region) compared to the perimeter. For light-dark exploration test, animals were placed in the light/dark chamber which is a square box (40 x 40 x 30 cm) equally divided into two compartments with a small open door joining the light and dark compartments. Their activity was tracked for 10 min with overhead camera and AnyMaze software. For elevated plus maze, the apparatus consisted of two opposing open arms (50 x 10 cm) and two opposing closed arms with roofless gray walls (40 cm) connected by a central square platform and positioned 50 cm above the ground. Mice were placed in the open arms facing an open arm, and their behavior was tracked for 5 min with an overhead camera and AnyMaze software.

Fluorescence-Activated Cell Sorting (FACS) Analysis

N2a cells were detached by incubating 5 min at 37°C in cell dissociation solution. After washing, samples were divided in two parts and half of the samples were kept in a minimal volume of PFN buffer (PBS supplemented with 1.5% FBS) for the non-permeabilized group. The remaining cells were re-suspended in PFN containing 0.05% saponin and gently rocked for 30 min at 4°C. Successive incubations with anti-HA antibody and secondary antibody conjugated to Alexa Fluor 488 were carried out at 4°C for 2 h and 1 h, respectively. Cells were analyzed in a FACSCalibur cytometer (BD Bioscience). Unstained cells were used as a control for background fluorescence. The geometric means of fluorescence intensity were obtained for

non-permeabilized and permeabilized samples, representing surface and total protein levels, respectively. The surface-to-total ratio was calculated for comparison.

Cell Biotinylation Assay

Cells were transfected with APP together with vector, or LRP6 and Mesd (a specialized chaperone required for proper folding of LRP6). After 24 h, cells were washed twice with PBS, and surface proteins were labeled with Sulfo-NHS-SS-Biotin (Pierce) under gentle shaking at 4°C for 30 min. Quenching solution (Pierce) was added to cells at 4°C, and washed twice with Tris-buffered saline. Cells were lysed in 500 µl of lysis buffer, incubated for 30 min on ice. To isolate biotin-labeled proteins, lysate was added to immobilized NeutroAvidin Gel and incubated for 60 min at room temperature. Gels were washed 5 times with wash buffer and incubated for 60 min with SDS-PAGE sample buffer including dithiothreitol. Surface and total proteins were analyzed by Western blot.

Western Blot and Co-immunoprecipitation

Samples were homogenized and incubated in PBS containing 1% TX-100, supplemented with protease inhibitor mix, 1 mM PMSF and 1 mM Na₃VO₄. Equal amounts of protein (by Bradford assay) were resolved by SDS/PAGE and transferred to PVDF membranes. After the membranes were blocked, proteins were detected with primary antibody. Membrane was probed with LI-COR IRDye secondary antibodies and detected using the Odyssey infrared imaging system (LI-COR). In some experiments, horseradish peroxidase-conjugated secondary antibody was visualized by ECL detection system (Pierce) and exposed to film. To detect low amount of proteins, some blots were incubated with horseradish peroxidase-conjugated secondary antibody, detected by SuperSignal West Femto Chemiluminescent Substrate (Pierce). For

immunoprecipitation, the lysates were pre-cleared using Protein A-agarose beads for 60 min at 4°C and immunoprecipitated overnight at 4°C using anti-myc or an anti-HA antibodies. The antibody-bound complexes were isolated by incubation with Protein A-agarose beads for 2 h. The precipitates were then washed three times with PBS and re-suspended in SDS sample buffer. For Western blot analysis, the following antibodies were used in this study: anti-LRP6 (Abcam; Cell Signaling), anti-PSD-95 (Cell Signaling), anti-synaptophysin (Millipore), anti-GluR1 (Millipore), anti-NMDAR1 (Millipore), anti-GFAP (Millipore), 6E10 (Covance) for total APP and sAPP α , anti-APP N-terminus antibody (IBL) for sAPP β , anti-APP C-terminal antibody (IBL) for APP-CTFs, anti- β -catenin (BD Bioscience), anti-calnexin (Cell signaling), anti-HA (Covance), anti-flag (Invitrogen), anti-alpha 1 Sodium Potassium ATPase (Abcam), anti-beta III tubulin (Abcam), anti-c-myc (Sigma) and anti- β -actin (Sigma) antibodies.

Immunofluorescence Staining

Cells were transfected with GFP-APP together with vector, or LRP6 and Mesd. Live cell surface staining was performed as described (Hoe et al., 2009; Megill et al., 2013). Briefly, live cultures were incubated with APP N-terminal antibody to specifically label surface APP, then lightly fixed for 5 min in 4% paraformaldehyde (4% PFA) (non-permeabilizing conditions). After fixation, antibody-labeled APP (surface APP) was detected with Alexa Fluor 555-conjugated secondary antibody for 60 min. The cells were then washed in PBS and permeabilized with cold methanol. Total levels of APP were measured by APP immunostaining after permeabilization. Images were collected using a Zeiss LSM510 confocal microscope (Carl Zeiss) and quantified as previously described (Hoe et al., 2009). For examining the morphology of primary neurons upon LRP6 knockdown, cells were stained with anti-MAP2 AlexaFluor488 conjugate (Millipore) for 2 h and the fluorescent images were captured with an inverted microscope (Olympus). For

immunofluorescence staining of synaptic markers, the following antibodies were used: Synaptophysin (Millipore), PSD-95 (Abcam), and MAP2 (Abcam), and AlexaFluor488-, 568-, and 647-conjugated secondary antibodies (Invitrogen). All images were acquired by a confocal laser-scanning fluorescence microscope (model LSM510 invert; Carl Zeiss, Germany).

Free β -catenin Pull-down Assay

To examine the strength of Wnt signaling in human brain samples, mouse brains, and cells expressing control or LRP6 shRNA, free β -catenin levels were determined using GST-E-Cadherin pull-down assay as previously described (Bafico et al., 1998).

RNA Isolation and Real-time PCR Analysis

Total RNA was isolated by using Trizol (QIAGEN) followed by RNeasy Mini kit (QIAGEN). For real-time PCR analysis, cDNA was synthesized from total RNA by SuperScript III reverse transcriptase (Invitrogen). All primer sets were purchased from SuperArray Biosciences (QIAGEN) except for human LRP5 qPCR primer sets which were from OriGene. Triplicate reactions were prepared using a 25- μ l mixture containing Platinum SYBR Green qPCR Super Mix UDG (Invitrogen). Real-time quantification was performed on iCycle iQ system (Bio-Rad) or HT7900 (ABI).

Supplemental References

Bafico, A., Gazit, A., Wu-Morgan, S.S., Yaniv, A., and Aaronson, S.A. (1998). Characterization of Wnt-1 and Wnt-2 induced growth alterations and signaling pathways in NIH3T3 fibroblasts. *Oncogene* 16, 2819-2825.

Chakrabarty, P., Ceballos-Diaz, C., Beccard, A., Janus, C., Dickson, D., Golde, T.E., and Das, P. (2010). IFN-gamma promotes complement expression and attenuates amyloid plaque deposition in amyloid beta precursor protein transgenic mice. *J Immunol* 184, 5333-5343.

Das, P., Verbeeck, C., Minter, L., Chakrabarty, P., Felsenstein, K., Kukar, T., Maharvi, G., Fauq, A., Osborne, B.A., and Golde, T.E. (2012). Transient pharmacologic lowering of Abeta production prior to deposition results in sustained reduction of amyloid plaque pathology. *Mol Neurodegener* 7, 39.

Guo, W., Keckesova, Z., Donaher, J.L., Shibue, T., Tischler, V., Reinhardt, F., Itzkovitz, S., Noske, A., Zurrer-Hardi, U., Bell, G., *et al.* (2012). Slug and Sox9 cooperatively determine the mammary stem cell state. *Cell* 148, 1015-1028.

Hoe, H.S., Lee, K.J., Carney, R.S., Lee, J., Markova, A., Lee, J.Y., Howell, B.W., Hyman, B.T., Pak, D.T., Bu, G., and Rebeck, G.W. (2009). Interaction of reelin with amyloid precursor protein promotes neurite outgrowth. *J Neurosci* 29, 7459-7473.

Li, Y., Lu, W., He, X., and Bu, G. (2006). Modulation of LRP6-mediated Wnt signaling by molecular chaperone Mesd. *FEBS Lett* 580, 5423-5428.

Liu, C.C., Pearson, C., and Bu, G. (2009). Cooperative folding and ligand-binding properties of LRP6 beta-propeller domains. *J. Biol. Chem.* 284, 15299-15307.

Liu, Q., Trotter, J., Zhang, J., Peters, M.M., Cheng, H., Bao, J., Han, X., Weeber, E.J., and Bu, G. (2010). Neuronal LRP1 knockout in adult mice leads to impaired brain lipid metabolism and progressive, age-dependent synapse loss and neurodegeneration. *The Journal of neuroscience : the official journal of the Society for Neuroscience* 30, 17068-17078.

Megill, A., Lee, T., DiBattista, A.M., Song, J.M., Spitzer, M.H., Rubinshtein, M., Habib, L.K., Capule, C.C., Mayer, M., Turner, R.S., *et al.* (2013). A tetra(ethylene glycol) derivative of benzothiazole aniline enhances Ras-mediated spinogenesis. *The Journal of neuroscience : the official journal of the Society for Neuroscience* 33, 9306-9318.

Schmidt, S.D., Nixon, R.A., and Mathews, P.M. (2005). ELISA method for measurement of amyloid-beta levels. *Methods Mol Biol* 299, 279-297.

Shinohara, M., Sato, N., Kurinami, H., Takeuchi, D., Takeda, S., Shimamura, M., Yamashita, T., Uchiyama, Y., Rakugi, H., and Morishita, R. (2010). Reduction of brain beta-amyloid (Abeta) by fluvastatin, a hydroxymethylglutaryl-CoA reductase inhibitor, through increase in degradation of amyloid precursor protein C-terminal fragments (APP-CTFs) and Abeta clearance. *J. Biol. Chem.* 285, 22091-22102.

Stewart, S.A., Dykxhoorn, D.M., Palliser, D., Mizuno, H., Yu, E.Y., An, D.S., Sabatini, D.M., Chen, I.S.Y., Hahn, W.C., Sharp, P.A., *et al.* (2003). Lentivirus-delivered stable gene silencing by RNAi in primary cells. *RNA* *9*, 493-501.

Tamai, K., Semenov, M., Kato, Y., Spokony, R., Liu, C., Katsuyama, Y., Hess, F., Saint-Jeannet, J.-P., and He, X. (2000). LDL-receptor-related proteins in Wnt signal transduction. *Nature* *407*, 530-535.

Tay, W.M., Bryant, J.G., Martin, P.K., Nix, A.J., Cusack, B.M., and Rosenberry, T.L. (2012). A mass spectrometric approach for characterization of amyloid-beta aggregates and identification of their post-translational modifications. *Biochemistry* *51*, 3759-3766.

Youmans, K.L., Leung, S., Zhang, J., Maus, E., Baysac, K., Bu, G., Vassar, R., Yu, C., and LaDu, M.J. (2011). Amyloid-beta42 alters apolipoprotein E solubility in brains of mice with five familial AD mutations. *J Neurosci Methods* *196*, 51-59.